ISSN 1070-3632, Russian Journal of General Chemistry, 2017, Vol. 87, No. 10, pp. 2351–2357. © Pleiades Publishing, Ltd., 2017.
Original Russian Text © A.Yu. Bugaeva, I.V. Loukhina, V.N. Filippov, B.N. Dudkin, 2017, published in Zhurnal Obshchei Khimii, 2017, Vol. 87, No. 10, pp. 1693–1700.

Ceramic Composite $[78ZrO_2–21CeO_2–Y_2O_3]/La_{0.85}Y_{0.15}Al_{11}O_{18}/Al_2O_3$. Microstructure and Properties

A. Yu. Bugaeva[a]*, I. V. Loukhina[a], V. N. Filippov[b], and B. N. Dudkin[a]

[a] Institute of Chemistry, Komi Science Center, Ural Branch, Russian Academy of Sciences,
ul. Pervomaiskaya 48, Syktyvkar, 167982 Russia
*e-mail: bugaeva-ay@chemi.komisc.ru

[b] Institute of Geology, Komi Science Center, Ural Branch, Russian Academy of Sciences, Syktyvkar, Russia

Received April 17, 2017

Abstract—A ceramic composite $[78ZrO_2–21CeO_2–Y_2O_3]/La_{0.85}Y_{0.15}Al_{11}O_{18}/Al_2O_3$ (zirconium dioxide submicroparticles stabilized by cerium and yttrium oxides), which consists of a matrix filled with layered submicroparticles of lanthanum hexaaluminate modified by yttrium oxide and reinforced by Al_2O_3 nanofibers, was obtained. Components of the composite were synthesized by the sol-gel method, except for Al_2O_3 nanofibers obtained by the electric explosion method. The microstructure and properties of the composite depend on the composition and methods of its formation and sintering. The composite is intended to be used as a construction material.

Keywords: composite, zirconium dioxide, lanthanum hexaaluminate, aluminum oxide, nanofiber, microstructure

DOI: 10.1134/S1070363217100164

Implantation of elements mechanically impeding the spread of cracks (by changing the direction of their movement or by blunting their vertices) into structure of ceramic materials improves ceramics properties. Initial size of powder particles substantially influences the material microstructure and such its properties as hardness, strength, plasticity, and behavior during prolonged operation.

Ceramic composites can be obtained on the principle of from the *bottom upwards* using already formed nanosize particles as the nanocomposite structure elements. To obtain the composites, it is useful to apply ultradisperse powders of simple and complex compositions as nucleating centers of grain formatuion, and to synthesize nanostructured materials on their basis [1, 2]. Nanosize particles obtained by the sol–gel method are successfully applied to the formation of such matrices [2–17]. The addition of particles with layered structure to the composite blend [3, 15, 18] and reinforcement of the ceramics by discrete or continuous fibers of various composition [3, 19–22] make it possible to minimize the growth of microcracks and fragility of the composite.

Zirconium-based materials are designed for continuous operation at high temperatures and mechanical loads as functional heat-shield coatings [7, 8] and heat-insulating materials [23]. They are also applied as implants in bone tissue [23–25], filling material in dentistry [26], catalysts [4–6, 27], solid oxide fuel cells [9, 28], gas sensors [29], and cutting tools [22, 30].

Increase in the strength of ceramics based on zirconium oxide (considering that the metastable tetragonal zirconium oxide modification t-ZrO_2 is unstable in the temperature range 20–1170°C) is reached by reducing grain size and introducing stabilizing additives of oxides of alkaline-earth and rare-earth elements. The choice of Y_2O_3 and CeO_2 as additives for stabilizing t-ZrO_2 was defined by optimal conditions for reaching stability of fluorite structure, namely, proximity of radii of Zr^{4+} (0.82 Å), triply charged Y^{3+} cation (0.97 Å), and rare-earth metal cation Ce^{4+} (0.88 Å). In addition, Y_2O_3 and CeO_2 are resistant to evaporation [31, 32].

The ability to stabilize nanoparticles of the phase t-ZrO_2 by Y_2O_3 and CeO_2 additives as structure-forming matrix phases and also as fillers in the t-ZrO_2/

Table 1. Dependence of t-ZrO_2 grain size on the composition and methods of synthesis and on molding and firing

Composite	Additive	Method of synthesis	Method of molding and firing	t-ZrO_2 grain size, μm
Al_2O_3/t-ZrO_2	–	Sol–gel	Cold isostatic pressing, firing at 1550°C, 4 h	0.020–0.200 [10]
Al_2O_3/t-ZrO_2	–	Sol–gel	Firing at 1250°C, 2 h	0.034–0.066 [31]
t-ZrO_2	Y_2O_3	Sol–gel	Firing at 1100–1400°C, 100 h	0.016–0.040 [7]
t-ZrO_2/Al_2O_3	Y_2O_3	Hydrothermal	Cold isostatic pressing at 300 MPa and subsequent sintering in air for 2 h at 1350–1550°C	<0.250 [26]
t-ZrO_2/Al_2O_3	Y_2O_3	Mechanochemistry	Hot pressing in a vacuum, 1500°C, 30 MPa	<0.270 [28]
t-ZrO_2/Al_2O_3/$LaAl_{11}O_{18}$	CeO_2	Hydrotermal	Cold isostatic pressing at 300 MPa and subsequent sintering in air 4 h at 1600–1625°C	2–4 [18]
Al_2O_3/t-ZrO_2	Y_2O_3, CeO_2	(1) Sol–gel (2) Mechanochemistry	Cold isostatic pressing at 350 MPa and subsequent sintering in air 4 h at 1600–1625°C	~0.110 [11] 0.540 [11]
t-ZrO_2 t-ZrO_2/Al_2O_3	Y_2O_3, CeO_2	Sol–gel	Firing at 1300°C, 5 h	0.24–1.68 [33] 0.21–0.58 [33]
t-ZrO_2/Al_2O_3	Y_2O_3, CeO_2	Sol–gel	Hot pressing in a vacuum at 1400–1450°C and 196 MPa in ArO_2 medium	0.35–0.4 [34]

Al_2O_3 composite was studied in a number of works (Table 1). The most effective way to increase t-ZrO_2 thermal stability is the introduction of Y_2O_3 and CeO_2 stabilizing additives into the a t-ZrO_2/Al_2O_3 composite [11, 33, 34]. In this case the temperature of conversion of the ZrO_2 tetragonal phase to the monoclinic phase ($t \rightarrow m$) is significantly reduced. The Al_2O_3 addition to the composite additionally inhibits the growth of t-ZrO_2 grains. This leads to an increase in elasticity modulus and strain energy of the composite.

We have studied the microstructure and properties of a new ceramic composite depending on composition and methods of its molding and firing. The composite consists of a matrix (zirconium dioxide submicroparticles stabilized by cerium and yttrium oxides) and a filler (lanthanum hexaaluminate submicroparticles modified by yttrium oxide). Composite components were obtained by the sol–gel method. The composite was reinforced by aluminum oxide nanofibers obtained by the electric explosion method.

The objects of the synthesis were ceramic filled composites **1** and **2** with ratios of components, mol %: $[78ZrO_2–21CeO_2–Y_2O_3] : La_{0.85}Y_{0.15}Al_{11}O_{18} = 78 : 22$ (**1**), $([78ZrO_2–21CeO_2–Y_2O_3] : La_{0.85}Y_{0.15}Al_{11}O_{18}) : Al_2O_3 = 99.75\ [78 : 22] : 0.25$ (**2**). The general scheme of obtaining the composite material and the procedures of preparation of sols of the composite material initial components are described in [3, 12–15, 35]. Mixed-composition sols and fibers were added simultaneously. The disperse phase of the resulting sol included all components of the composite material. The composite microstructure was designed in the stage of sol → gel → xerogel transitions of the colloidal system with a complex oxide composition (Scheme 1).

We have proposed the scheme of formation of particles of the dispersed phase with a complex composition starting from the solubility of metal hydroxides in the system (cerium hydroxide $Ce(OH)_4$ solubility in water, –log (SP)$Ce(OH)_4$ 54.80), is considerably lower than those of zirconium, aluminum, yttrium, and lanthanum hydroxides {–log (SP)$Zr(OH)_4$ 52.00; –log (SP)$Al(OH)_3$ 32.00; –log (SP)$Y(OH)_3$ 24.50; –log (SP)$La(OH)_3$ 22.24 [36]}. The formation and growth of nucleating particles of the dispersed phases under joint hydrolysis of salts of these metals occur at pH values corresponding to oversaturation of

Scheme 1. Composite preparation.

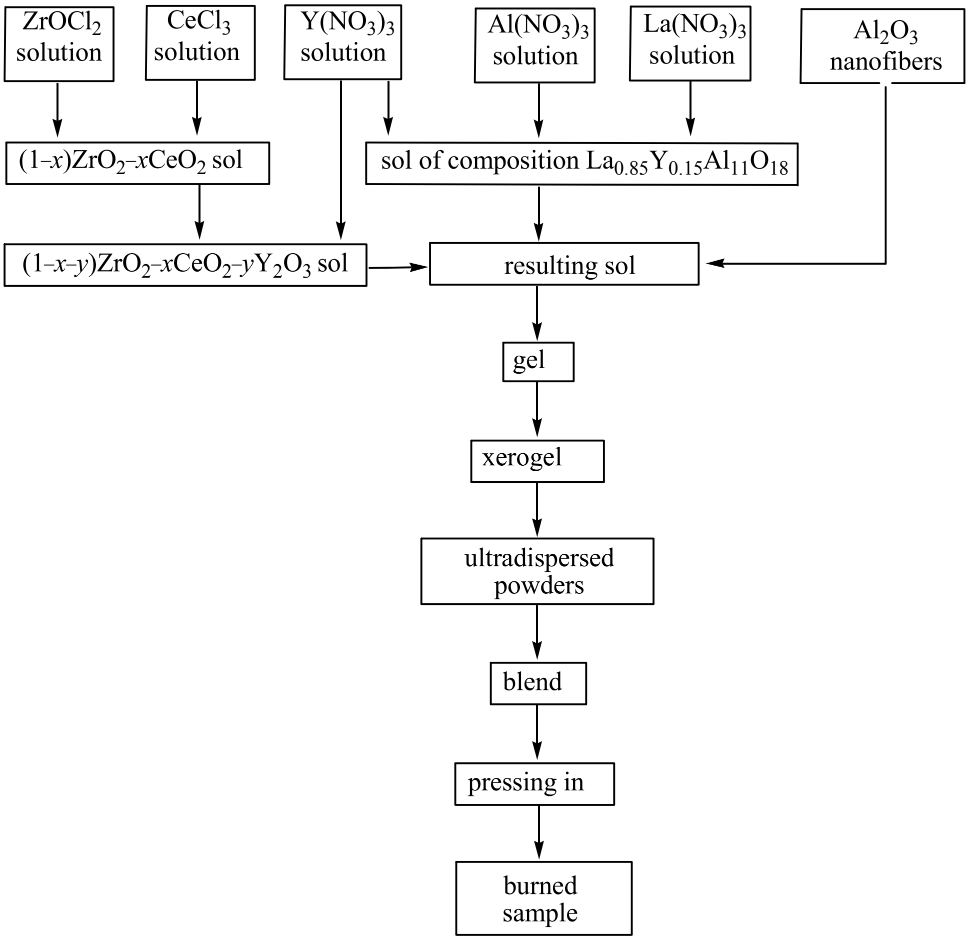

the mixed solutions. When the Al_2O_3 nanofibers are added to the sol with a mixed composition, hydrated CeO_2 particles are sorbed on the surface of Al_2O_3 nanofibers. As pH of the dispersion medium increases, more soluble particles of hydrated ZrO_2, Al_2O_3, Y_2O_3, and La_2O_3 are formed. So-called shell of a mixture of hydrated metal oxides is formed. Thus, Al_2O_3 fibers possessing excessive surface energy [1, 37] serve as nucleating centers of agglomerated particles (grains) of the phase with a complex composition consisting of a mixture of hydrated metal oxides.

Integration of resulting colloidal systems and Al_2O_3 nanofibers in one system with saving aggregative and sedimentation stability allowed us to ensure distribution uniformity of the components in bulk xerogel.

According to the data of thermal analysis and differential scanning calorimetry (TG–DSC), it was found that joint addition of Al_2O_3 nanofibers, modifying Y_2O_3 and CeO_2 additives, and hydrated metal oxides (in accordance with the filler composition $La_{0.85}Y_{0.15}Al_{11}O_{18}$) reduces the temperature of formation of the low-temperature modifications t'-ZrO_2 and m'-ZrO_2 up to 280–410°C (unlike 480°C [4] and 467°C [10]). The addition of Al_2O_3 nanofibers to the composite material leads to a decrease in the temperature of formation of cubic cerium oxide (c-CeO_2), which modifies zirconium dioxide solid solutions (based on the t-ZrO_2 and m-ZrO_2 phases). The temperature of obtaining ultradispersed powders of composite material **2** is reduced by approximately 140°C (Table 2).

According to the X-ray phase analysis (XRD), the composites are presented by zirconium oxide of monoclinic m-ZrO_2 (ICSD 82543) and tetragonal t-ZrO_2 (ICSD 68781) modifications, $(x - y)ZrO_2–(x - y)CeO_2–yY_2O_3$ solid solution ($x = 0.22$, $y = 0.1$), and lanthanum hexaaluminate $LaAl_{11}O_{18}$ (ICSD 38395) [38].

In composite **2** obtained by the semidry pressing method with afterburning by the ceramic technology (method *1*) 40% of t'-ZrO_2 was formed and the size of

Table 2. Thermal effects occurring on obtaining composite materials **1** and **2**[a]

Processes	Temperature of thermal effects (maxima), °C	
	1	**2**
Water desorption	121	100
Decomposition of metal hydroxides	207	132, 200
Decomposition of NH_4NO_3	260	250
Decomposition of NH_4Cl	281	271
Formation of m'-ZrO_2 and t'-ZrO_2	280–410	280–410
Formation of c-CeO_2	521	509
Formation of m-ZrO_2	978	928
Transformation m-$ZrO_2 \rightarrow t$-ZrO_2	1160	1150
Formation of $La_{0.85}Y_{0.15}Al_{11}O_{18}$	1200	1200
Formation of solid solutions	1218, 1264, 1346, 1382	1218, 1246, 1357, 1370
Temperature of the mass loss end	700	557

[a] m'-ZrO_2 and t'-ZrO_2 are low-temperature monoclinic and tetragonal zirconium dioxide modifications, respectively; c-CeO_2 is cubic cerium dioxide modification; m-ZrO_2 is high-temperature monoclinic zirconium dioxide modification; t-ZrO_2 is high-temperature tetragonal zirconium dioxide modification.

t-ZrO_2 crystallites reduced approximately to one-fourth of its original size. In composites **1** and **2** obtained by hot pressing (method *2*), fully stabilized t-ZrO_2 was formed at the temperature lower by 50–75°C and pressure lower by an order than in the work [18]. The addition of Al_2O_3 nanofibers to composite 2 (composite **2**, method *2*) leads to a twofold increase in the size of t-ZrO_2 crystallites, whereas size of t-ZrO_2 crystallites in composite 2 obtained by method *1* is less approximately by half (Table 3).

Thus, two requirements of the metastable t-ZrO_2 synthesis and stabilization are fulfilled in both methods of molding and firing: reduction of the size of t-ZrO_2 crystallites from submicrons [16, 18, 26, 28] to nanometers [7, 10, 30, 39, 40] (but no more than 30 nm [7, 10]) and limitation of the possibility of their agglomeration.

Table 3. Fractions and size of t-ZrO_2 phase crystallites in the composite matrix

Method of molding and firing	Composite	x_t, %	d_t, nm
1	**1**	100	16.9
	2	40	4.3
2	**1**	100	4.9
	2	100	8.4

Fibers Al_2O_3 (LLC “Novosibirsk nanomaterials”) before heat consisted of a mixture of ν- and δ-Al_2O_3 phases with the cross-section size up to 10–50 nm.

To prepare the composite material, Al_2O_3 fibers after heat treatment were used, the phase composition of which is represented by α-Al_2O_3 phases (not less than 95%) and θ-Al_2O_3 (no more than 5%) with a cross-section up to 200–300 nm.

The dependence of formation of the composite microstructure on the composition and procedures of their molding and firing was studied by the scanning electron microscopy (SEM) method. The microstructure of the resulting composites is homogeneous in distribution of all components. Crystallites of the ZrO_2 matrix and their solid solutions with cerium and yttrium oxides have a pseudo-cubic shape with the fluorite structure. Their elemental composition corresponds to the samples in points *a* (Table 4). Crystallites of the filler $LaAl_{11}O_{18}$ are of a plate shape with the β-Al_2O_3 layered structure. The elemental composition corresponds to the samples in points *b* (Table 4). They are distributed in the form of small agglomerates. Joint addition of Al_2O_3 nanofibers and CeO_2 and Y_2O_3 additives leads to levelling grain boundaries of the matrix.

The elemental composition (at. %) determined by the SEM/EDS method for the surface of samples of composites **1** and **2** prepared by procedures *1* and *2* is presented in Table 4. According to the X-ray spectral

Table 4. SEM/EDS data[a] on the elemental composition (at. %) in various points of sample surface of composites **1** and **2** obtained by procedures *1* and *2*

Sample	Al	La	Y	Zr	Ce	Hf	O
1 (*1a*)	6.02	1.19	3.75	23.24	0.83	0.27	64.70
1(*1b*)	34.93	2.88	0.40	1.36	1.24	–	60.19
2 (*1a*)	–	0.23	1.31	30.89	0.39	0.23	66.23
2 (*1b*)	36.04	1.49	0.09	0.29	1.66	0.11	60.12
2 (*1c*)	29.20	1.49	–	6.41	1.61	0.01	61.28
1 (*2a*)	35.63	2.88	0.03	0.12	1.32	–	60.02
1 (*2b*)	5.02	1.29	4.02	23.78	1.13	–	64.76
2 (*2a*)	34.98	2.62	0.15	0.84	1.26	0.07	60.08
2 (*2b*)	6.54	1.33	4.04	22.68	0.87	–	64.54
2 (*2c*)	28.34	2.54	0.91	5.85	1.18	–	61.17

[a] Ratio of components corresponds to the theoretical composition in terms of metal oxides.

analysis of the distribution of elements in the composite 2 sample (sintered by procedure *1*), various metal elements (Zr , Ce, Al, and La) [Table 4, samples **2**(1*c*) and **2**(2*c*)] are present in white grains formed on nucleation centers of Al_2O_3 nanofibres.

Size of matrix and filler grains in composite **2** containing fibers decreases in two and more times for both methods of obtaining composites, which points to the participation of fibers in the formation of composite microstructure. For the same chemical and phase composition method *2* makes it possible to obtain composite 2 with a grain size three times smaller than in the case of method *1* (Table 5).

The results of studying physicomechanical properties of composites are presented in Table 6. In the case of both methods of obtaining composites **1** and **2** their low porosity results from Y_2O_3 sintering action [14], whereas the high density of the composite samples (no less than 0.7 of the X-ray density [41]) and the increase in hardness after Vickers is defined by both phase composition and influence of compaction and sintering at various preparation procedures.

Thus, [$78ZrO_2$–$21CeO_2$–Y_2O_3]/$La_{0.85}Y_{0.15}Al_{11}O_{18}$/$Al_2O_3$ (**2**) ceramic composite containing fully stabilized *t*-ZrO_2 was obtained by hot pressing; grain size of the composite is three times less and the hardness is higher by 25% compared to the composite prepared by dry pressing with subsequent firing. It was possible to obtain such a composite by using composite materials prepared by the sol–gel method (Al_2O_3 nanofibers were obtained by the electric explosion method). The fundamental distinctive feature of the offered method of obtaining composite is the scheme of formation of particles of the disperse complex-composition phase based on growth of disperse sol phase particles formed on the surface of Al_2O_3 nanofibers.

EXPERIMENTAL

Components of the complex ceramic composite were synthesized by the sol–gel method. Nanofibers of Al_2O_3 were obtained from an aluminum wire by the electric explosion method [1, 41]. The size of the nanofibers was estimated by the specific surface area determined by the Brunauer, Emmett, and Teller method and by the laser granulometry data (LLC "Novosibirsk nanomaterials").

Sintered composite samples were obtained by the semidry pressing method with subsequent firing according to the ceramic technology (method *1*) and by uniaxial hot pressing (method *2*).

Method *1*. Samples were formed by the dry pressing method with uniaxial loading. Wax in CCl_4 was used as a technological binder. Firing in the range from 500 to 1600°C was carried out stepwise in air in electric furnaces with carborundum heaters. Sintered composite samples were obtained at 1600°C and the heating rate of 10 deg/min with isothermal exposure for 20 h in air.

Method *2*. Samples were molded in graphite molds at a pressure of 15 MPa. Temperature condition included heating to 1550°C at a rate of 30 deg/min and isothermal exposure for 2 h.

Table 5. Influence of composition and methods of molding and firing ultradispersed powders on the grain size of composites **1** and **2**

Forming and firing method	Composite	Size of grains of $78ZrO_2/21CeO_2/Y_2O_3$ matrix, μm	Size of grains of $La_{0.85}Y_{0.15}Al_{11}O_{18}$ filler, μm	Size of grains formed on Al_2O_3 nanofibers, μm
1	**1**	1.8–3.3	2.5–16.0	
	2	0.5–1.5	0.7–3.0	0.300–1.0
2	**1**	0.3–1.0	2.5–2.9	
	2	0.3–0.8	1.2–1.3	0.100–0.250

Table 6. Physicomechanical properties of ceramic composites

Molding and firing method	Composite	Apparent density, g/cm^3	Relative density, %	Water absorption, %	Porosity, %	Vickers hardness, HPa
1	**1**	5.302±0.002	86.4±0.1	0.7±0.1	3.5±0.1	(11.0±0.5)–(13.0±0.5)
	2	5.769±0.002	94.0±0.1	0.4±0.1	2.3±0.1	(11.0±0.5)–(14.0±0.5)
2	**1**	5.056±0.002	82.3±0.1	0.2±0.1	1.0±0.1	(15.0±0.5)–(17.0±0.5)
	2	5.735±0.002	93.4±0.1	0.1±0.1	0.5±0.1	(16.0±0.5)–(18.0±0.5)

Thermal transformations of the composite material were studied by the TG-DSC method on a NETZSCH STA 409 PC instrument. The measurements were carried out in a dynamic mode from 25 up to 1400°C at a heating rate of 10 deg/min in alundum crucibles in air. Phase composition of the composite was determined by the X-ray phase analysis data on a Shimadzu XRD-6000 X-ray diffractometer (CuKα radiation). Fractions of the t-ZrO_2 phase (x_t) in the composite were determined using values of intensities of the reflection from the plane (111), 2θ 30.5° for t-ZrO_2 and from the planes (111), 2θ 28.4° and (11I), 2θ 31.6° for m-ZrO_2. Values of x_i were calculated by the following formula [30].

$$x_t = I_t(111)/(I_m(111) + I_m(11\mathrm{I}) + I_t(111)).$$

The average crystallite size of the t-ZrO_2 phase (d_t) in composite samples was determined by broadening of the line corresponding to the (111) reflection, 2θ 30.5°, the calculations being fulfilled by the Scherrer formula [30].

Microstructure of Al_2O_3 nanofibers was studied on a JEM-2010 high-resolution transmission electron microscope (LLC "Novosibirsk nanomaterials"). Microstructure of composite samples was studied on a JSM-6400 JEOL scanning electron microscope. The X-ray spectral analysis of composite samples was performed on a Link-ISIS-300 X-ray spectrometer. Values of apparent density, water absorption, and open porosity of composite samples were determined by the water absorption method according to GOST 2409-95. Vickers hardness of composite samples was determined by GOST 2999-75.

ACKNOWLEDGMENTS

The work was carried out using equipment of the "Chemistry" Centers for joint usage of Institute of chemistry and the "Geology" Center of the Institute of geology of the Komi Science Center of the Ural Branch of the Russian Academy of Sciences.

The authors express their gratitude to V.V. Troshkov (LLC "Novosibirsk nanomaterials") for the submission of aluminum oxide nanofibers, to P.V. Istomin and A.V. Nadutkin (Institute of chemistry of the Komi Science Center of the Ural Branch of Russian Academy of Sciences, and to D.A. Shushkov for measurement of Vickers hardness (Institute of geology of the Komi Science Center of the Ural Branch of Russian Academy of Sciences).

REFERENCES

1. Burtsev, V.A., Kalinin, N.V., and Luchinskii, A.V., *Elektricheskii vzryv provodnikov i ego primenenie v elektrofizicheskikh ustanovkakh* (Electric Explosion of Conductors and its Application in Electrophysical Installations), Moscow: Energoatomizdat, 1990.
2. *Belaya kniga po nanotekhnologiyam: issledovaniya v oblasti nanochastits, nanostruktur i nanokompozitov v Rossiiskoi Federatsii* (White Book on Nanotechnology: Research in the Field of Nanoparticles, Nanostructures,

and Nanocomposites in the Russian Federation), Moscow: Izd. LKI, 2008.

3. Dudkin, B.N., Bugaeva, A.Yu., Zainullin, G.G., and Filippov, V.N., *Inorg. Mater*., 2010, vol. 46, no. 4, p. 445. doi 10.1134/S0020168510040229
4. *Pakhomov, N.A., Nauchnye osnovy prigotovleniya katalizatorov. Vvedenie v teoriyu i praktiku* (Scientific Basis for the Preparation of Catalysts: an Introduction to Theory and Practice), Novosibirsk: SO RAN, 2011.
5. Gavrilova, N.N. and Nazarov, V.V.*, Colloid J.,* 2011, vol. 73, no. 1, p. 28. doi 10.1134/S1061933X11010054
6. Huang, W., Wang, Z., Xu, J., Fan, X., Wang, Y., Zou, B., and Cao, X., *Corros. Sci*., 2013, vol. 74, p. 22. doi 10.1016/j.corsci.2013.04.003
7. Viazzi, C. Bonino, J.P., Ansart, F., Barnabé, A., *J. Alloys Products Compd*., 2008. vol. 452, no. 2, p. 377.
8. Yao, Y.B., Yao Z.J., and Zhou, Y.J., *J. Sol-Gel Sci. Technol*., 2016, vol. 80, p. 612. doi 10.1007/s10971-016-4172-3
9. Khrushcheva, A.A., *Cand. Sci. (Chem.) Dissertation*, Moscow, 2016.
10. Vol'khin, V.V., Zharnyl'skaya, A.L., Kazakov, D.A., and Leont'eva, G.V., *Izv. Vyssh. Uchebn. Zaved., Khim. Khim. Tekhnol*., 2010, vol. 53, no. 7, p. 3.
11. Naga, S.M., Abdelbary, E.M., Awaad, M., El-Chhaer, Y.I., Abd-Elwahab, H.S., *Ceram. Int.,* 2013, vol. 39, p. 1835. doi 10.1016/j. ceramint. 2012.08.031
12. Galakhov, A.V. and Shevchenko, V.Ya., *Ogneupory,* 1994, no. 1, p. 8.
13. Viravathana, P. and Marr, D.W.M., *J. Colloid Interface Sci*., 2000, vol. 221, no. 2, p. 301. doi 10.1006/ jcis.1999.6603
14. Bugaeva, A.Yu., *Cand. Sci. (Chem.) Dissertation*, Chelyabinsk, 2003.
15. Dudkin, B.N., Bugaeva, A.Yu., and Zainullin, G.G., *Konstr. iz Kompoz. Mater*., 2010, no. 1, p. 9.
16. Messing, G.L. and Kumagai, M., *J. Am. Ceram. Soc*., 1989, vol. 72, no. 1, p. 40. doi 10.1111/j.1151-2916.1989.tb05950
17. Podzorova, L.I., Shvorneva, L.I., Il'icheva, A.A., Alad'ev, N.A., and Pen'kova, O.I., *Inorg. Mater*., 2013, vol. 49, no. 4, p. 376. doi 10.7868/S00023
18. Fujii, T., Muragaki, H., Hatano, H., and Hirano, S., *Ceram. Trans*., 1991, vol. 22 (Ceram. Powder Sci. 4), p. 693.
19. Brandon, D. and Kaplan, U., *Mikrostruktura minerialov. Metody issledovaniya* (Microstructure of Materials. Research methods), Moscow: Tekhnosfera, 2004.
20. Shevchenko, V.Ya. and Barinov, S.M., *Tekhnicheskaya keramika* (Technical Ceramics), Moscow: Nauka, 1993.
21. Barinov, S.M. and Shevchenko, V.Ya., *Prochnost' tekhnicheskoi keramiki* (The Strength of Technical Ceramics), Moscow: Nauka, 1996.
22. Garshin, A.P., Gropyanov, V.M., Zaitsev, G.P., and Semenov, S.S., *Keramika dlya mashinostroeniya* (Ceramics for Mechanical Engineering), Moscow: Nauchtekhizdat, 2003.
23. Kulkov, S., Litvinova, L., Kalatur, E., and Buyakov, A., *J. Phys*., 2015, no. 1, p. 602. doi 10.1088/1742-6596/602/1/012028
24. Igarashi, K., Nakahara, K., Haga-Tsujimura, M., Kobayashi, E., and Watanabe, F.*, Dent. Mater. J*., 2015, vol. 34, no. 5, p. 692. doi 10.4012/dmj.2014-361
25. Hallmann, L., Ulmer, P., Reusser, E., Louvel, M., and Hämmerle, Ch.H.F., *J. Eur. Ceram. Soc.,* 2012, vol. 32, p. 4091. doi 10.1016/j.jeurceramsoc.2012.07.032
26. Zhang, F., Vanmeensel, K., Inokoshi, M., Batuk, M., Hadermann, B., Meerbeek, V., Naert, I., and Vleugels, J., *J. Eur. Ceram. Soc*., 2014, vol. 34, p. 2453. doi 10.1016/j.jeurceramsoc.2014.02.026
27. Reddy, B.M., Saikia, P., and Bharali, P., *Catal. Surv. Asia*, 2008, vol. 12, p. 214. doi 10.1007/s10563-008-9053-5
28. Bansal, N.P. and Zhu, D., *Ceram. Int*., 2005, vol. 31, p. 911. doi 10.1016/j.ceramint.2004.09.018
29. Heiroth, S., Frison, R., Rupp, J.L.M., Lippert, T., Meier, B.E.J., Müller, L. Gubler, E., Döbelie, M., Conder, K., Wokaun, A., and Gauckler, L.*, Solid State Ionics*, 2011, vol. 191, p. 12. doi 10.1016/ j.ssi.2011.04.002
30. Sarkar, D., Adak, S., and Mitra, N.K., *Composites (A),* 2007, vol. 38, p. 124. doi 10.1016/ j.compositesa.2006.01.005
31. Konsztowicz, K.J. and Langlois, R., *J. Mater. Sci.,* 1996, vol. 31, p. 1633. doi 10.1007/BF00357875
32. Yoshimura, M., Oh, S., Sando, M., and Niihara, K.*, J. Alloys Compd*., 1999, vol. 290, nos. 1–2, p. 284. doi 10.1016/S0925-8388(99)00213-3
33. Yin, S., Fujishiro, Y., Uchida, S., and Sato, T., *J. Supercrit. Fluids*, 1998, vol. 13, p. 363. doi 10.1016/ S0896-8446(98)00073-4
34. Hirano, M. and Inada, H., *J. Am. Ceram. Soc*., 1991, vol. 74, no. 3, p. 609. doi 10.1111/j.1151-2916.1991.tb04067.x
35. Bugaeva, A.Yu., Loukhina, I.V., Belyi, V.A., and Dudkin, B.N., *Russ. J. Gen. Chem*., 2014, vol. 84, no. 2, p. 190. doi 0.1134/S1070363214020042.
36. *Spravochnik khimika* (Chemist's Handbook), Nikol'skii, B.P., Ed., Moscow: Khimiya, 1965, vol. 3.
37. Il'in, A.P., Gromov, A., A., and Yablunovskii, G.V.*, Fizika Goreniya i Vzryva*, 2001, vol. 37, no. 4, p. 58.
38. https://icsd.fiz-karlsruhe.de/search/.
39. Zavodinskii, V.G. and Chibisov, A.N., *Phys. Solid State*, 2006, vol. 48, no. 2, p. 363. doi 10.1134/ S1063783406020296
40. Karagedov, G.R. and Avakumov, E.G., *Khimiya v Interesakh Ustoichivogo Razvitiya*, 2011, no. 19, p. 521.
41. Khasanov, O.L. and Bikbaeva, Z.G., *Nanostrukturnaya keramika, poroshkovye tekhnologii kompaktirovaniya konstruktsionnykh materialov* (Nanostructural Ceramics, Powder Technologies of Compacting Structural Materials), Tomsk: FGAOU VO NI TPU, 2009.